ON THE ANGLE OF ARRIVAL STATISTICS IN TYPICAL URBAN CHANNELS

A. U. H. Sheikh and Saad Muhammed Al-Ahmadi.

Telecommunication Research Laboratory,
Electrical Engineering Department, King Fahd University of Petroleum & Minerals
Dhahran 31261, Saudi Arabia
Broadband Communications and Wireless Systems (BCWS) research centre
Department of Systems and Computer Engineering,
Carleton University, Colonel By Drive, Ottawa, Canada K1S 5B6
(asrarhaq@kfupm.edu.sa , saahmadi@sce.carleton.ca)

Abstract: Geometrical modeling can be used to characterize mobile radio channels in spatial domain. In this paper, we introduce a geometrical model for wideband typical urban channels. In this model, the effective scatterers confined to a circular area around the mobile are modeled by a bivariate Gaussian distribution and the angle of arrival probability density function is derived for different system bandwidths, radii of scattering area, and the distance between the mobile and base stations.

Index terms - Typical Urban Channels, Geometric Modeling, Wideband Elliptical model, Gaussian distribution, Angle of Arrival.

I. INTRODUCTION

Space-time processing schemes (such as 2-D RAKE receivers) are being introduced in CDMA-DS based mobile radio systems to reduce delay spread, multipath fading and co-channel interference and hence to increase the system capacity [1, 2]. However, the optimal design of such schemes requires the development of more appropriate spatial channel models. The channel models in [3, 4] which where used to compute the spatial correlations at the base station (BS), are essentially narrowband models and are not appropriate for wideband (frequency selective) channels. In [5], a wideband channel for bad urban channels was introduced and it was shown that the spatially and temporally distinct paths do have different AoA statistics at the BS and consequently different spatial correlation coefficients. In this paper, a geometric wideband model for typical urban areas is proposed; the AoA pdf's at both the BS and the MS are derived.

II. CHANNEL GEOMETRY AND SCATTERER'S DISTRIBUTION.

The appropriate model of the wideband typical urban (TU) channel is shown in fig. 1. In this elliptical model, the BS and the MS are located at the foci of concentric ellipses where the *i*th ellipse corresponds to the *i*th multipath component. The major axis of the *i*th ellipse is given as [6]

$$a_i = \frac{c\left(\tau_0 + (2\cdot i - 1)\cdot T_c\right)}{2} \quad (1)$$

Where c is the speed of light, $\tau_0 = D/c$ and T_c is the system chip-rate.

The effective scatterers are assumed to lie in a circle of a radius R around the mobile. Since the significance of the scatterers is expected to reduce as the distance from the mobile increases, then the bi-variate Gaussian distribution is the appropriate distribution [7]. So, the scatterer's pdf can be expressed in polar coordinates as

$$p(r_m, \theta_m) = \frac{1}{2\pi}\exp\left(\frac{r_m^{\ 2}}{\sigma_m^{\ 2}}\right) \quad (2)$$

where r_m denotes the distance as measured from the mobile to a scatterer 'S' as shown in fig. 1. The joint pdf of scatterers at the BS can be expressed in polar coordinates as

$$p(r_b, \theta_b) = \frac{r_b}{2\pi\sigma_m^{\ 2}}\exp\left[\frac{-\left(r_b^{\ 2} - 2r_b D\cos\theta + D^2\right)}{2\sigma_m^{\ 2}}\right] \quad (3)$$

Where r_b denotes the distance as measured from the BS to a scatterer 'S'. The variance, σ_m^2, is dependent on the physical layout of scatterers and the transmitted power of the mobile. However, assuming that the radius of significant scatterers around the MS ranges from 60m to 300m [7], and assuming that the Gaussian pdf is significant over the range of 2.5 to 3 times, the standard deviation σ_m will range from 20-100 m.

III. THE AoA PDF'S:

A. At the BS:

The pdf of the AoA of the received wave-field in LOS TU channels can be modeled using the concept of mixed distributions where the total pdf can be expressed as the sum of two parameterized pdf's

$$p_t(\theta_b) = (1-\sqrt{1-m^{-1}})\cdot p(\theta_b) + \sqrt{1-m^{-1}}\cdot\delta(\theta_b-\theta_{LOS}),\ m\ge 1, -\pi\le\theta\le\pi \quad (4)$$

where m is the Nakagami fading parameter and θ_{LOS} is the AoA of the LOS component. The term $p(\theta_b)$ stands for the pdf of the diffused component at the BS that is due to the mobile scatterers. In (4), the contribution of the scatterers around the BS and the double scattering term were neglected due to the high density of scatterers around the mobile and high attenuation in urban environments, the probability of significant contribution of distant scatterers is negligible.

The AoA pdf's of the diffused component can be derived as

$$p(\theta_b) = \int_{r_{b1}(\theta)}^{r_{b2}(\theta)} p(r_b,\theta_b)\,dr_b \quad (5)$$

where $r_{b1}(\theta)$ and $r_{b2}(\theta)$ are the intersection points of the line θ_b = constant and the scatterers region and are dependent on the radius of the effective scatterer's circle and the system chip-rate.

Case I: the area of scatterers is limited to the first ellipse only:

This scenario takes place in narrowband systems where T_c is relatively large with a small radius of circle of scatterers. For example, in IS-95, the chip-rate T_c =1/1.2288 MHz results in a major axis of the first ellipse a_1=D+122 m. So, if R≤122 m, then the circle of scatterers will be confined to the first ellipse. Substituting (4) in (5) and using the polar coordinate expression of the circle of scatterers centered at D

$$r_b(\theta_b) = D\cos\theta_b \pm\sqrt{D^2\cos^2\theta_b - D^2 + R^2} \quad (6)$$

The AoA pdf can be derived as in (7). The parameters in (7) are given as

$$\begin{aligned}
p(\theta_b) &= \frac{1}{2\sqrt{2\pi}\sigma_m}.D\cos\theta_b.\exp\left[\frac{D^2(\cos^2\theta_b-1)}{2\sigma_m^2}\right]\cdot\left[\operatorname{erf}\left(\frac{K_2-D\cos\theta_b}{\sqrt{2}\sigma_m}\right)+\operatorname{erf}\left(\frac{K_1-D\cos\theta_b}{\sqrt{2}\sigma_m}\right)\right]\\
&+\left(\frac{1}{2\pi}\right)\cdot\exp\left(\frac{-D^2}{2\sigma_m{}^2}\right)\cdot\left\{\exp\left[\frac{-K_1(K_1-2D\cos\theta_b)}{2\sigma_m{}^2}\right]-\exp\left[\frac{-K_2(K_2-2D\cos\theta_b)}{2\sigma_m{}^2}\right]\right\},|\theta_b|\le\beta_1
\end{aligned}$$

$$\begin{aligned}
p(\theta_b) &= \frac{1}{2\sqrt{2\pi}\sigma_m}.D\cos\theta.\exp\left[\frac{D^2(\cos^2\theta-1)}{2\sigma_m^2}\right]\cdot\left[\operatorname{erf}\left(\frac{R_1-D\cos\theta}{\sqrt{2}\sigma_m}\right)+\operatorname{erf}\left(\frac{K_1-D\cos\theta}{\sqrt{2}\sigma_m}\right)\right]\\
&+\left(\frac{1}{2\pi}\right)\cdot\exp\left(\frac{-D^2}{2\sigma_m{}^2}\right)\cdot\left\{\exp\left[\frac{-K_1(K_1-2D\cos\theta)}{2\sigma_m{}^2}\right]-\exp\left[\frac{-R_1(R_1-2D\cos\theta)}{2\sigma_m{}^2}\right]\right\}\\
&+\frac{1}{2\sqrt{2\pi}\sigma_m}.D\cos\theta.\exp\left[\frac{D^2(\cos^2\theta-1)}{2\sigma_m^2}\right]\cdot\left[\operatorname{erf}\left(\frac{K_3-D\cos\theta}{\sqrt{2}\sigma_m}\right)+\operatorname{erf}\left(\frac{R_1-D\cos\theta}{\sqrt{2}\sigma_m}\right)\right]\\
&+\left(\frac{1}{2\pi}\right)\cdot\exp\left(\frac{-D^2}{2\sigma_m{}^2}\right)\cdot\left\{\exp\left[\frac{-R_1(R_1-2D\cos\theta)}{2\sigma_m{}^2}\right]-\exp\left[\frac{-K_3(K_3-2D\cos\theta)}{2\sigma_m{}^2}\right]\right\},|\theta_b|\le\beta_2
\end{aligned}$$

(7)

$$K_1(\theta_b) = D\cos\theta_b - \sqrt{D^2\cos^2\theta_b - D^2 + R^2} \quad (8)$$

$$K_2(\theta_b) = D\cos\theta_b + \sqrt{D^2\cos^2\theta_b - D^2 + R^2} \quad (9)$$

and

$$\beta_1 = \sin^{-1}\left(\frac{R}{D}\right) \quad (10)$$

The plot of the AoA pdf for T_c = 1/1.2288 MHz, D= 400 m, R=100 m and σ_m =30 m is shown in fig. 2.

Case II: the region of scatterers extends beyond the first ellipse:

This scenario takes place in wideband systems, for example T_c =1/3.84 MHz, where the high resolution will result in the extension of the scatterer's area beyond the first ellipse as shown in fig. 1. Now, to

Top

derive the AoA pdf of the first path, the integral in (5) has be separated into two parts (corresponding to two regions) as

$$p(\theta) = \int_{r_{b1}(\theta)}^{R_1} p\left(r_b, \theta\right) dr_b + \int_{R_1}^{r_{b2}(\theta)} p\left(r_b, \theta\right) dr_b$$

(11)

where $r_{b1}(\theta)$ can be expressed using (6) and $r_{b2}(\theta)$ is determined using the polar coordinate expression of an ellipse of a major axis a

$$r_b(\theta_b) = \frac{\frac{a^2}{4} - D^2}{a - 2D\cos(\theta_b)} \qquad (12)$$

The resulting AoA pdf is given as in (13)

$$p(\theta_b) = \frac{1}{2\sqrt{2\pi}\sigma_m}.D\cos\theta_b.\exp\left[\frac{D^2\left(\cos^2\theta_b - 1\right)}{2\sigma_m^2}\right]\cdot\left[\operatorname{erf}\left(\frac{K_3 - D\cos\theta_b}{\sqrt{2}\sigma_m}\right) + \operatorname{erf}\left(\frac{K_2 - D\cos\theta_b}{\sqrt{2}\sigma_m}\right)\right]$$
$$+\left(\frac{1}{2\pi}\right)\cdot\exp\left(\frac{-D^2}{2\sigma_m{}^2}\right)\cdot\left\{\exp\left[\frac{-K_2(K_2 - 2D\cos\theta_b)}{2\sigma_m{}^2}\right] - \exp\left[\frac{-K_3(K_3 - 2D\cos\theta_b)}{2\sigma_m{}^2}\right]\right\}, |\theta_b| \le \beta_3$$

(13)

Where

$$K_3(\theta_b) = \frac{\frac{a_1{}^2}{4} - D^2}{a_1 - 2D\cos(\theta_b)} \otimes \qquad (14)$$

The distance R_1 and the angle β_2 are found by solving equation corresponding to the intersection of the circle of scatterers with the first ellipse.

The extension of the scatterers region beyond the first ellipse will introduce the second path. However, the derivation of the AoA pdf of the second path is dependent on the channel geometry. When the region of scatterers extends beyond the first ellipse only (does not intersects with the second ellipse), then the lower limit of the integral in (5) will be given by the curve of the fist ellipse and the upper limit is given by the curve of the circular region as shown if fig. 1. The AoA pdf can be expressed as in (15) where

$$\beta_3 = \sin^{-1}\left(\frac{R}{D}\right) \qquad (16)$$

The plots of the AoA pdf for different values of the radius of scatteres R are shown in fig 3 and 4. Those plots show that the significance of the second path increases as R increases as a consequence of having more scatterers beyond the first ellipse. Also, it can be noticed that the second path has a smoother pdf and more angular spread, which will result in lower spatial correlations at the BS.

IV. CONCLUSIONS

In this paper, a new geometrical model for typical urban channels is introduced. In this elliptical model, the region of scatterers is extended beyond the first ellipse and the AoA pdf,s are derived for both narrowband and wideband CDMA systems. The derived AoA pdf's can be used to compute the resulting spatial correlations at the BS.

ACKNOWLEDGEMENT

The authors acknowledge the support of KFUPM to carry out the research reported in this paper.

REFRENCES

[1] Special Issue on Smart Antennas, IEEE Personal Commun, vol. 5, no.1, Feb. 1998.

[2] M. Fang, 2-D RAKE Transceiver for IMT-2000 Systems, Ph.D. Dissertation, Tsinghua Univ. China, 1999.

[3] W. Y. C. Lee, "Effects on correlation between two mobile radio base-station antennas," *IEEE Trans. on Commun*, vol. 21, no. 11, pp. 1214- 1224, November 1973.

[4] J. Salz and J. H. Winters, "Effect of fading correlation on adaptive arrays in digital mobile radio," *IEEE Trans. Veh. Technol*. vol. 43, no. 4, pp. 1049-1057, Nov. 1994.

[5] Al-ahmadi, Saad and Asrar, U.H. Sheikh, "Spatial domain modeling of microcellular systems operating in multipath Nakagami channels," *IEEE PIMRC*, pp. 1942-1946. 2002.

[6] J. C. Liberti & T. S. Rappaport, Smart Antennas for Wireless Communications: IS-95 and Third Generation CDMA Applications. Prentice Hall. 1999.

[7] J. Fuhl, A. F. Molisch, and E. Bonek, "Unified channel model for mobile radio systems with smart antennas," IEE *Proc. Radar, Sonar*, Navig, vol. 45, pp. 32-41, 1998.

Top

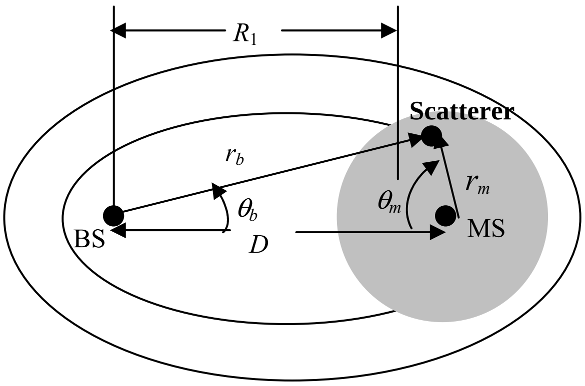

Fig.1 The channel geometry for a two path model

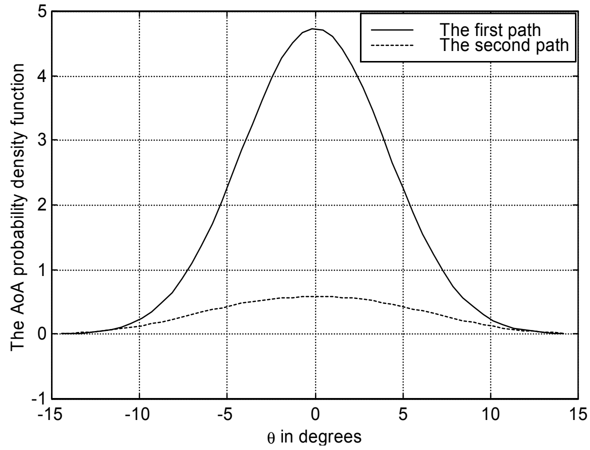

Fig. 3. The AoA pdf of the two paths for m=1, T_c = 1/3.84 MHz, D= 400 m, R=100 m and σ_m =30 m.

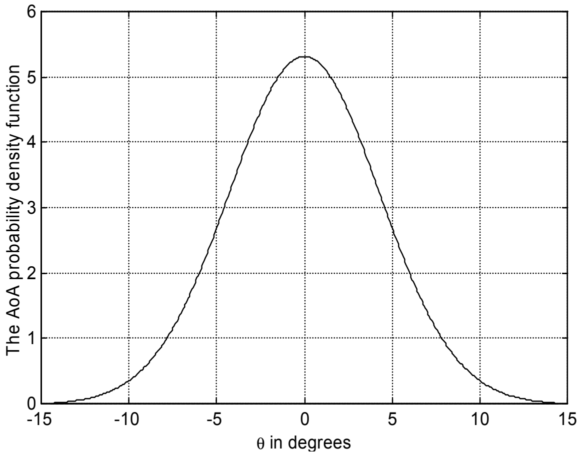

Fig. 2. The AoA pdf of the single path for m=1, T_c = 1/1.2288 MHz, D= 400 m, R=100 m and σ_m =30 m.

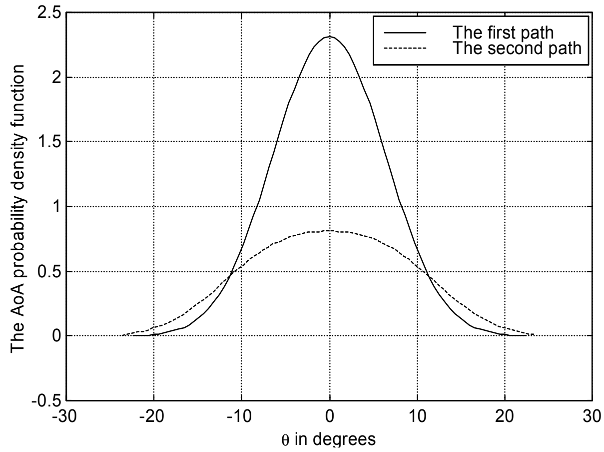

Fig. 4. The AoA pdf of the two paths for m=1, T_c = 1/3.84 MHz, D= 400 m, R=160 m and σ_m =50 m.

Top